

## Ion-Surface Interactions, and Electronically Stimulated Desorption of Physisorbed Atoms

R. E. Walkup, Ph. Avouris, and N. D. Lang

*IBM Research Division, Thomas J. Watson Research Center, P.O. Box 218, Yorktown Heights, New York 10598*

R. Kawai

*Department of Chemistry, University of California, La Jolla, California 92093*

(Received 11 July 1989)

Diabatic potential-energy curves for  $\text{Ar}^+$  and  $\text{Kr}^+$  interacting with a metal surface are reported. At intermediate distances, the attractive force is considerably smaller than the classical result for an ion attracted to its image charge. This has a substantial impact on the dynamics of electronically stimulated desorption, and on the Franck-Condon broadening of photoemission lines. Quantum effects on ion motion are considered, and the validity of a classical treatment is discussed.

PACS numbers: 79.20.-m, 61.45.+s, 68.45.-v, 73.20.Hb

In a variety of dynamical processes involving the interaction of positive ions with solid surfaces, the form of the ion-surface interaction potential plays a crucial role. At large distances from the surface the interaction is well represented by a point charge attracted to its image charge. However, at the small distances relevant for most surface dynamical processes, there is overlap between the ion and surface charge densities, and the potential will deviate from the ideal image form. The shape of the potential-energy (PE) surface is of fundamental importance to such processes as electronically stimulated desorption,<sup>1-4</sup> the position and width of adsorbate lines observed by photoemission spectroscopy,<sup>5</sup> and the forces experienced by ions in scattering or sputtering experiments. Desorption due to ionization of physisorbed noble-gas atoms is of particular interest here because the yields and kinetic energy distributions of the desorbed particles are sensitive to the ion-surface potentials, and detailed experimental measurements have recently become available.<sup>6</sup>

In this Letter, we present calculations of diabatic PE curves for the noble-gas ions  $\text{Ar}^+$  and  $\text{Kr}^+$  interacting with a metal surface, and we use these to examine the dynamics of noble-gas desorption caused by ionization of the physisorbed atoms. Desorption proceeds by a mechanism proposed by Antoniewicz.<sup>7</sup> Ionization of the atom creates a hole in a level located below the bottom of the metal valence band. This hole can be filled by Auger neutralization,<sup>8</sup> with a rate that is small enough to allow substantial motion on the ionic PE curve. The positive ion is expected to be attracted *toward* the surface by image-like forces. If sufficient kinetic energy is gained on the ionic curve, then upon neutralization, the atom will recoil from the surface and desorb. Since noble-gas atoms on metal surfaces provide a good model system, this subject has attracted considerable attention.<sup>6,9-14</sup> However, in previous treatments, the ionic PE curve has been assumed to be an image potential (with added short-range repulsion); and this results in an unsatisfactory level of agreement between experiment and theory.

We will show that the PE curves reported here lead to an improved description of the desorption process. In addition, we discuss the implications of these potentials for the Franck-Condon broadening of photoemission lines, and we investigate the nature of ion motion by comparing quantal and classical descriptions of electronically stimulated desorption.

Diabatic ion-surface PE curves were calculated using the local-density-functional (LDF) approach of Lang and Williams.<sup>15</sup> In this treatment the metal is regarded as a medium with a planar, semi-infinite, uniform, positive background charge density, with an electron density in the bulk,  $n_e$ , characterized by  $r_s = (3/4\pi n_e)^{1/3}$ . Wave functions for the adatom-metal system are calculated in a self-consistent manner, using the Kohn-Sham density-functional theory;<sup>16</sup> the details of the method are provided in Ref. 15. This method has proven useful for calculations of the ground-electronic-state PE curves for chemisorbed<sup>15</sup> and physisorbed<sup>17</sup> atoms, and of diabatic PE curves for electronically excited states formed by the creation of a hole in a level located below the bottom of the metal valence band.<sup>18,19</sup> In the current calculations, the metal is specified by  $r_s = 3$  bohrs. This provides a reasonable description of a variety of metals including Ag and Au, and (more approximately) Ru and Cu. The calculations give the change in charge density and the total electronic energy due to the presence of an ion at some specified distance from the positive background edge. The PE curve is obtained by evaluating the total electronic energy for a sequence of ion-surface distances.

The results for  $\text{Ar}^+$  and  $\text{Kr}^+$  are shown in Fig. 1 along with an image potential,  $V_{\text{image}} = e^2/[4(x - x_i)]$ , where  $x - x_i$  is the distance from the image plane.<sup>20</sup> The most important feature of the PE curves is that for the distances relevant for physisorption (4-6 bohrs in Fig. 1), the attractive force is substantially *less* than that predicted by an image potential. Moreover, the discrepancy is not substantially reduced by adding to the image potential a physically reasonable repulsive term such as the repulsion for the corresponding neutral atom. The re-

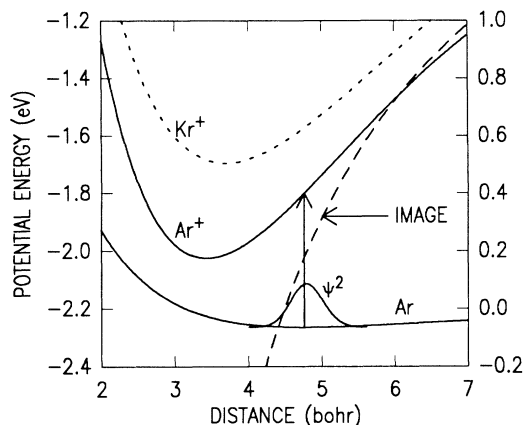


FIG. 1. Potential-energy curves (left scale) for  $\text{Ar}^+$  and  $\text{Kr}^+$  interacting with a metal surface are shown together with an image potential. Distance is measured from the positive background edge of the metal. The ground-state curve (right scale) for Ar is shown along with the probability density for the lowest bound state.

duced attractive force has a number of consequences. For example, in photoemission studies of adsorbates, the Franck-Condon contribution to the linewidth depends on the slope of the ionic PE curve at the minimum in the ground-state well.<sup>5</sup> The calculated Franck-Condon widths for Ar (at 50 K) are  $\approx 460$  meV for an image potential and  $\approx 210$  meV for the LDF potentials. For Ar monolayers on Pt(111) the experimental width is  $\approx 300$  meV FWHM,<sup>21</sup> measured with an instrument resolution of  $\approx 90$  meV. An image potential clearly overestimates the width. In contrast, the LDF results appear to be in reasonable agreement with the data, given the uncertainties in the intrinsic lifetime-broadened width and in the manner in which the instrument, lifetime, and Franck-Condon widths add.

The physical origin of the reduced attractive force can be seen from the charge-density contours shown in Fig. 2. When a positive ion enters the near-surface region, the imagelike charge density is initially attracted toward the ion. There is also a repulsive interaction between the electrons bound to the ion and the imagelike charge density, which results in a polarization of the ion density away from the surface and corresponding local depression in the imagelike density. As the ion moves closer to the surface, the imagelike charge density is pushed toward the metal. Thus the effective image plane moves inward as the ion approaches; and the attractive force is reduced compared to an estimate using a fixed image plane. There is also a small amount of charge transferred from the metal into large radius orbitals surrounding the ion. This reduces the effective charge, which also reduces the imagelike interaction. For  $\text{Ar}^+$  and  $\text{Kr}^+$ , this mixing with excited neutral states is rather small in the near-surface region, and the most important effect is the displacement of the imagelike charge by the

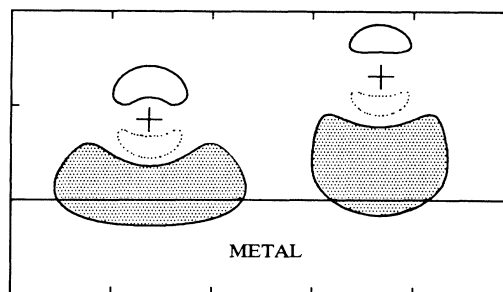


FIG. 2. Charge-density-difference contours  $\rho_{\text{ion+metal}} - (\rho_{\text{bare metal}} + \rho_{\text{free ion}})$  are shown for  $\text{Ar}^+$  at distances of 4.25 bohrs (left) and 6.5 bohrs (right). The horizontal line marks the positive background edge of the metal, and the ion position is indicated (plusses). The contour densities are  $\pm 0.001$  bohr<sup>-3</sup> (solid-dotted line). As the ion approaches the surface, the imagelike density (shaded area) is pushed toward the metal.

incoming ion.

Now we turn to a discussion of motion on these PE curves due to ionization of a physisorbed atom. In order to make a decisive comparison with experimental data, both classical and quantal treatments of the dynamics were carried out. In the quantal approach, a term  $-iW(x)$  is added to the potential energy to describe the net effect of Auger neutralization, as discussed by Brenig and co-workers.<sup>22,23</sup>  $W(x)$  is directly related to the neutralization rate,  $\Gamma(x) = 2W(x)/\hbar$ . The probability for neutralization to result in a given eigenstate,  $\Psi_f$ , of the ground-state (neutral) system is<sup>24</sup>

$$P(\Psi_f) = \int_0^\infty dt |\langle \Psi_f | \Gamma(x)^{1/2} | \phi_i(x,t) \rangle|^2,$$

where  $\phi_i(x,t)$  is the time-dependent wave packet describing nuclear motion on the ionic PE curve and  $P$  is the probability. The wave packet  $\phi_i(x,t)$  was obtained by direct numerical solution<sup>25</sup> of the time-dependent Schrödinger equation subject to the condition that at  $t=0$   $\phi_i(x,t)$  is given by the lowest bound-state wave function of the physisorption well, as appropriate for a Franck-Condon transition to the ionic PE curve at  $T=0$  K. The experimental quantities of interest are the yield,  $Y$ , and the kinetic energy (flux) distribution,  $F(E)$ , of the desorbed neutral atoms. These were evaluated by the relationships  $Y = \int_0^\infty dk P(\Psi_k)$  and  $F(E) \propto kP(\Psi_k)$ , where  $\Psi_k$  is a continuum state characterized by a kinetic energy  $E = (\hbar k)^2/2m$ . PE curves for physisorbed atoms were obtained by the LDF method.<sup>17</sup> The only "free" parameters in our treatment are those that characterize the Auger neutralization rate:  $\Gamma(x) = \Gamma_0(x/x_0)^2 \times \exp[-b(x-x_0)]$ , where  $x$  is the distance measured from the outermost internuclear plane and  $x_0$  is the location of the bottom of the physisorption well. The Auger matrix element scales as the square of metal wave functions averaged over the adsorbate position; thus  $\Gamma(x)$

should be roughly proportional to the square of the metal electron density versus the distance from the surface,<sup>26</sup> and the exponential factor  $b$  is expected to be  $\sim 5 \text{ \AA}^{-1}$ .

A comparison of the calculated kinetic distribution for Ar and the recent measurements of Steinacker and Feulner<sup>6</sup> is shown in Fig. 3. Good agreement is obtained by choosing Auger parameters of  $\hbar\Gamma_0=0.03 \text{ eV}$  and  $b=6 \text{ \AA}^{-1}$ . For these values, the calculated yield is  $Y \approx 12\%$ , which is smaller than the experimental<sup>6</sup> estimate of  $\sim 64\%$ . The experimental value is based on the assertion that the yield is unity for transitions that form  $\text{Ar}^{+2}$ . However, LDF calculations for Ar with *two* holes in the  $3p$  level indicate that such states are effectively neutral, i.e.,  $\text{Ar}^*(3p^4 4s^2)$ , due to charge transfer from the metal into the  $n=4$  levels. Therefore, the states formed by double ionization should quickly decay by an intra-atomic Auger process,<sup>27</sup> resulting in a neutral desorption yield below unity. Hence the experimental yield may be too large. Also, the calculated yield is too small because of the neglect of inelastic effects in the model. Using classical trajectory calculations and an embedded-atom treatment of the metal,<sup>28</sup> we estimate that  $\sim 20\%$  of the Ar kinetic energy is transferred to metal phonons. If an allowance is made for inelastic effects of this magnitude, good agreement with the energy distribution can be obtained with yield estimates of  $Y \sim 20\%$ . Better agreement should come with more accurate absolute data and/or additional improvements in the model. In particular, interactions between adsorbates and energy loss due to electron-hole excitations should be included. The experimental energy distribution could also be fitted using a classical image potential. However, the resulting neutralization parameters are not realistic:  $\hbar\Gamma_0 \approx 2 \text{ eV}$ ,  $b \approx 20 \text{ \AA}^{-1}$ . The width is much larger than experimental widths,<sup>21</sup> and the variation of the rate with distance is too rapid to be physically meaningful. In addition, the yield estimate is considerably smaller,  $Y \approx 2.8\%$ . Thus the LDF potentials considerably improve the description of electronically stimulated desorption. However, a more detailed model including inelastic effects is needed for accurate quantitative results.

For a basic understanding of the desorption problem, it is important to examine the role of quantal versus classical dynamics.<sup>23,29,30</sup> In order to directly compare quantal and classical descriptions, it is useful to express the Schrödinger equation in fluid-flow form,

$$\frac{\partial \rho}{\partial t} + \frac{\partial}{\partial x}(\rho v) = -\Gamma(x)\rho,$$

$$\frac{\partial J}{\partial t} + \frac{\partial}{\partial x}(Jv) = \frac{\rho}{m}[F_C + F_Q] - \Gamma(x)J,$$

where  $\rho$  and  $J$  are the probability and current densities, and  $v=J/\rho$ ,  $F_C = -\partial V/\partial x$ , and

$$F_Q = \frac{\hbar^2}{4m} \left[ \frac{\partial^3 \ln(\rho)}{\partial x^3} + \frac{\partial \ln(\rho)}{\partial x} \frac{\partial^2 \ln(\rho)}{\partial x^2} \right].$$

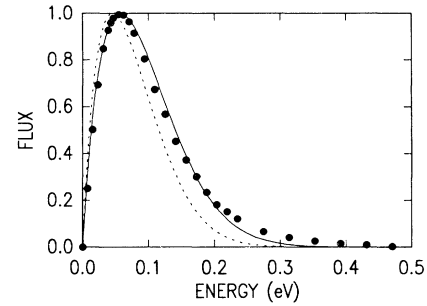


FIG. 3. Energy distributions for neutral argon desorbed via the Antoniewicz mechanism. The data of Steinacker and Feulner (Ref. 6) are shown (dots) along with quantal (solid line) and classical (dashed line) predictions. The theoretical curves use the same initial distribution and Auger-decay parameters. All distributions are scaled to a peak value of 1.0.

$F_C$  is the classical force and  $F_Q$  is the quantal "force." The time-dependent Schrödinger equation, including damping via a local complex potential, is identical to the classical equations of motion for a fluid of noninteracting particles with a spatially varying loss rate, except for the addition of a quantal force term  $F_Q$  which depends on the probability density  $\rho$ . At  $T=0 \text{ K}$  the initial distribution is determined by the ground-state wave function,  $\psi_0$ , in accordance with the Franck-Condon principle. The same initial conditions can be employed in a classical description by choosing  $\rho = |\psi_0|^2$  and  $v=0$ . One can then estimate the difference between classical and quantal *dynamics* by comparing  $F_C$  and  $F_Q$ . For a Gaussian distribution,  $F_Q = \hbar^2(x-x_c)/mw^4$ , where  $x_c$  is the centroid position and  $w$  is the width (half width at  $1/e$  points of the probability density). The quantal force tends to spread the distribution. Upon ionization of physisorbed Ar,  $F_C \approx -0.5 \text{ eV \AA}^{-1}$ , whereas  $F_Q \approx 0.03(x-x_c)/w \text{ eV \AA}^{-1}$ . Thus the classical force dominates, and the initial motion will be essentially classical. Roughly speaking, classical dynamics is good when  $|F_C| > |F_Q|$  over the relevant time period. For  $\text{Ar}^+$ , this criterion is approximately satisfied; and it is a fair approximation to treat ion motion classically starting with the quantum mechanically correct initial distribution function, as, for example, in the model of Moog, Unguris, and Webb.<sup>10</sup> A comparison of classical and quantal predictions of the Ar energy distribution is shown in Fig. 3. The quantal result is somewhat broader, in better agreement with experiment. The classical prediction for the yield was  $\approx 12\%$ , in agreement with the quantal result. The importance of quantum effects in the dynamics depends critically on the value of the classical force resulting from the electronic transition. If the transition is to a steeply sloped excited-state PE curve, then the classical force will be large and the motion will be essentially classical.

In summary, we have presented self-consistent calculations of diabatic PE curves for noble-gas ions interacting

with metal surfaces. For intermediate distances from the surface, the attractive force is considerably less than that predicted by the classical image potential. The LDF potentials provide an improved description of desorption stimulated by the ionization of physisorbed atoms, and Franck-Condon broadening in photoemission spectroscopy. The role of quantum effects on ion motion was also investigated. For noble-gas desorption, a classical treatment of ion motion is qualitatively correct provided that the width of the initial distribution is accounted for. However, a quantal approach is needed for an accurate description of the kinetic energy distributions.

We thank P. Feulner (Technische Universität München) for providing experimental data prior to publication.

- 
- <sup>1</sup>M. L. Knotek, Rep. Prog. Phys. **47**, 1499 (1984).  
<sup>2</sup>T. E. Madey, D. E. Ramaker, and R. L. Stockbauer, Annu. Rev. Phys. Chem. **35**, 215 (1984).  
<sup>3</sup>*Desorption Induced by Electronic Transitions III*, edited by R. H. Stulen and M. L. Knotek (Springer-Verlag, Berlin, 1988).  
<sup>4</sup>Ph. Avouris and R. E. Walkup, Annu. Rev. Phys. Chem. **40**, 173 (1989).  
<sup>5</sup>J. W. Gadzuk, S. Holloway, C. Mariani, and K. Horn, Phys. Rev. Lett. **48**, 1288 (1982).  
<sup>6</sup>E. Steinacker and P. Feulner, Phys. Rev. B (to be published).  
<sup>7</sup>P. R. Antoniewicz, Phys. Rev. B **21**, 3811 (1980).  
<sup>8</sup>H. D. Hagstrum, Phys. Rev. **96**, 336 (1954).  
<sup>9</sup>Q. H. Zhang, R. Gomer, and D. R. Bowman, Surf. Sci. **129**, 535 (1983).

- <sup>10</sup>E. R. Moog, J. Unguris, and M. B. Webb, Surf. Sci. **134**, 849 (1983).  
<sup>11</sup>P. Feulner, T. Müller, A. Puschmann, and D. Menzel, Phys. Rev. Lett. **59**, 791 (1987).  
<sup>12</sup>Z. W. Gortel, H. J. Kreuzer, P. Feulner, and D. Menzel, Phys. Rev. B **35**, 8951 (1987).  
<sup>13</sup>Z. W. Gortel, H. J. Kreuzer, P. Feulner, and D. Menzel, in Ref. 3, p. 173.  
<sup>14</sup>D. R. Jennison, E. B. Stechel, and A. R. Burns, in Ref. 3, p. 167.  
<sup>15</sup>N. D. Lang and A. R. Williams, Phys. Rev. B **18**, 616 (1978).  
<sup>16</sup>W. Kohn and L. J. Sham, Phys. Rev. **140**, A1133 (1965).  
<sup>17</sup>N. D. Lang, Phys. Rev. Lett. **46**, 842 (1981).  
<sup>18</sup>N. D. Lang, J. K. Norskov, and B. I. Lundqvist, Phys. Scr. **34**, 77 (1986).  
<sup>19</sup>Ph. Avouris, R. Kawai, N. D. Lang, and D. M. Newns, Phys. Rev. Lett. **59**, 2215 (1987); J. Chem. Phys. **89**, 2388 (1988).  
<sup>20</sup>N. D. Lang and W. Kohn, Phys. Rev. B **7**, 3541 (1973).  
<sup>21</sup>G. Schönhense, B. Kessler, N. Müller, B. Schmiedeskamp, and U. Heinzmann, Phys. Scr. **35**, 541 (1987).  
<sup>22</sup>W. Brenig, Z. Phys. B **23**, 361 (1976).  
<sup>23</sup>P. Schuck and W. Brenig, Z. Phys. B **46**, 137 (1982).  
<sup>24</sup>This relation can be obtained from the more general results of Z. W. Gortel, R. Teshima, and H. J. Kreuzer, Phys. Rev. B **37**, 3183 (1988), when a local energy-independent optical potential is used to describe neutralization.  
<sup>25</sup>M. D. Feit, J. A. Fleck, Jr., and A. Steiger, J. Comput. Phys. **47**, 412 (1982).  
<sup>26</sup>N. D. Lang and W. Kohn, Phys. Rev. B **1**, 4555 (1970).  
<sup>27</sup>Data for related states of Ar are given by R. P. Madden, D. L. Ederer, and K. Codling, Phys. Rev. **177**, 136 (1969).  
<sup>28</sup>S. M. Foiles, M. I. Baskes, and M. S. Daw, Phys. Rev. B **33**, 7983 (1986).  
<sup>29</sup>Gortel, Teshima, and Kreuzer, Ref. 24.  
<sup>30</sup>W. Hübner and W. Brenig, Z. Phys. B **74**, 361 (1989).